INTERNATIONAL JOURNAL OF HYDROGEN ENERGY 39 (2014) 8590–8595

Available online at www.sciencedirect.com

ScienceDirect

journal homepage: www.elsevier.com/locate/he

Hydrogen absorption in Pd thin-films

S. Ramos de Debiaggi [a,b], E.A. Crespo [a], F.U. Braschi [a], E.M. Bringa [b,c], M.L. Alí [a], M. Ruda [d,e,*]

[a] Dpto. de Física, Fac. de Ingeniería, Universidad Nacional del Comahue, Buenos Aires 1400, 8300 Neuquén, Argentina
[b] CONICET, Argentina
[c] Instituto de Ciencias Básicas, Universidad Nacional de Cuyo, 5500 Mendoza, Argentina
[d] Centro Atómico Bariloche, 8400 Bariloche, Argentina
[e] Centro Regional Universitario Bariloche, Universidad Nacional del Comahue, Argentina

ARTICLE INFO

Article history:
Received 2 December 2013
Accepted 3 January 2014
Available online 31 January 2014

Keywords:
Hydrogen in metals
Thin-films
Pd
Monte Carlo
Molecular dynamics

ABSTRACT

Hydrogen absorption isotherms for Pd thin films were modeled at atomistic scale by Monte Carlo (MC) simulation in the TPμN ensamble and by Molecular Dynamics (MD) simulations at 300 K. The interaction among atoms was modeled by embedded atom method (EAM) potentials. Simulated samples consisted of monocrystalline nanofilms with different thickness (2–8 nm) and two crystallographic surface orientations, (001) and (111). The isotherms were compared to bulk Pd and a few available experimental results. Instead of the plateau corresponding to the α-β PdH equilibrium in the bulk, the isotherms at nanofilms show a two-plateaux behavior: a small one corresponding to a surface–subsurface hydride formation, and a larger one for the subsequent bulk hydride formation. This is strongly correlated with the atomic stress distribution induced within the thin film. The equilibrium pressures at the isotherms depend on the thin-film thickness, with pressure being larger for thicker films. The isotherms of the (001) films display lower equilibrium pressures than those for (111) films.

1. Introduction

Pd thin films have a wide field of applications as hydrogen sensors, H-selective membranes for hydrogen purification and materials for electrodes used in batteries [1 and references within,2–4]. This is because Pd can easily absorb a relatively large amount of hydrogen which has a high mobility within the Pd lattice [2]. Most films are deposited onto substrates and can be single crystals, polycrystals or amorphous depending on the deposition conditions. The presence or absence of a substrate, the thickness of the films, and the mean size of their microstructure (which may range from nanometers to micrometers) are all factors that influence thin film's mechanical and absorption properties.

Computer simulations of unsupported (111), (001) and (011) thin films of gold, using an embedded atom (EAM) potential were performed by Wolf [5], to analyze surface-stress-induced structure and elastic behavior of thin films. Streitz et al. [6] performed similar calculations on thin films of several fcc

* *Corresponding author*. Centro Atómico Bariloche, 8400 Bariloche, Argentina. Tel.: +54 294 4445278; fax: +54 294 4445190.
E-mail addresses: margaritaruda@yahoo.com, ruda@cab.cnea.gov.ar (M. Ruda).
0360-3199/$ – see front matter
http://dx.doi.org/10.1016/j.ijhydene.2014.01.013

metals (Ni, Cu, Ag and Au) and calculated the (111) and (001) surface stress as a function of the number of atomic layers. They attributed the unusual elastic behavior of the (001) films to their instability with respect to a (011) shear, which enables them to close pack their surface. Reconstruction from the (001) to the (111) orientation have been observed in Au and other suspended fcc metal nanofilms at a critical film thickness [7]; however in 4*d* metals (Rh, Pd and Ag) it does not occur unless an external stress is applied to the surface [8].

In general, a free metal film would expand in all three directions upon H absorption [9]. However, there is an interplay between the mechanical stresses already present in thin films, the H-induced stress modifications and the generation of microstructural defects that can change isotherms and phase boundaries, as well as leading to plastic deformations [1,10,11].

Absorption–desorption Pd–H isotherms were measured gravimetrically by Feenstra et al. [12] on thin Pd films deposited on a quartz substrate, at 382 K, 471 K and 519 K. The film's thicknesses were 300 nm and 50 nm. For the 50 nm samples they obtained slightly sloped, narrower plateaux than for the 300 nm samples, which behaved very similar to the bulk. The thin film's critical temperature was also reduced by about 100 K with respect to the bulk Pd–H. The hysteresis effect was smaller on the thinner films for all temperatures. Similar results were obtained by Pivak et al. [13] who measured Pd–H isotherms for Pd films supported on sapphire with and without an intermediate Ti layer using the Hydrogenography technique described in Ref. [11].

In previous works we have modeled H absorption isotherms for Pd nanoparticles of different sizes and shapes [14–16]. We used embedded atom (EAM) empirical interatomic potentials and Monte Carlo grand canonical simulations. We found that at low H concentrations, H prefers to go to the subsurface sites and for non-spherical particles H is first absorbed near vertices, then at edges, and finally on facets. This sequence correlates to stress concentration sites and a first sloped plateau or shoulder in the isotherm was observed corresponding to the formation of a hydride in the outer shell of clusters. At higher pressures, H was absorbed in the core of the clusters leading to a second, flatter "bulk" like plateau.

The purpose of this work is to study the effects of thickness and stress distribution on the hydrogen absorption properties of Pd unsupported monocrystalline nanofilms with two crystallographic orientations: (111) and (001). The paper is organized as follows: we begin by describing the computational methodology leading to the simulation of the H absorption isotherms at the atomistic scale and to the calculation of the stress per atom distribution along the nanofilms. Then we present and analyze the effects of the crystallographic orientations and film thicknesses on the resulting isotherms.

2. Numerical methods

We performed atomistic simulations using the embedded atom method (EAM) potentials developed by Zhou et al. [17] for representing the interatomic interactions amongst Pd and H atoms. We found these potentials are reliable to model the entire hydrogen composition range and predict reasonably well the miscibility gap of the Pd–H system. We have verified that this potential gives surface energies which are within 1%–20% of *ab initio* results (see Table 1). Isotherms were calculated by applying the Monte Carlo (MC) technique in the ($TP\mu_H N_M$) statistical ensemble, where the temperature T, pressure P, hydrogen chemical hydrogen potential μ_H and number of metal atoms N_M, are kept constant [18,19]. The system is open to the interchange of H from a reservoir at μ_H, which is in contact with a constant P reservoir and a constant T reservoir. Although from statistical thermodynamics, the values of μ_H and the H pressure can easily be connected at low H pressures (see Ref. [16]), we prefer to represent the isotherms as μ_H–composition functions, because they are still valid at large H concentrations [20].

In the present Monte Carlo simulations we perform four different trial jumps: (1) change of the volume of the system; (2) particle relaxation; (3) creation and (4) destruction of an H atom at random sites along the Pd fcc sample. The program executes up to approximately 35,000 steps per atom in the sample; 5% are trials type (1), 45% of the trials are type (2) and the rest of the moves are distributed evenly between the other two trials. The program simulates the H absorption process; at each μ_H the sample is hydrogenated reaching an average

Table 1 – Surface and hydrogen absorption energies for Pd (111) and (001). The H absorption and segregation energies were calculated considering a surface hollow site or an octahedral site at the subsurface. Coverage: θ = H atoms/Pd surface atoms.

Surface orientation	Surface energy (mJ/m^2)	Segregation energy (eV/atom)	Absorption energy (eV)	H site
(111)	1939	−1.10	−1.42	Surface
	1220 [25]	−1.18 [26]	($\theta = 0.0018$)	
	1920 [26]		−0.7 ($\theta = 1$)	
			−2.88 [27]	
		−1.09	−1.41	Subsurface
			−2.58 [27]	
(001)	1977	−1.05	−1.34	Surface
	1370 [25]	−1.05 [26]	($\theta = 0.0018$)	
	2326 [26]		−0.7 ($\theta = 1$)	
			−2.81 [27]	
		−0.71	−1.00	Subsurface

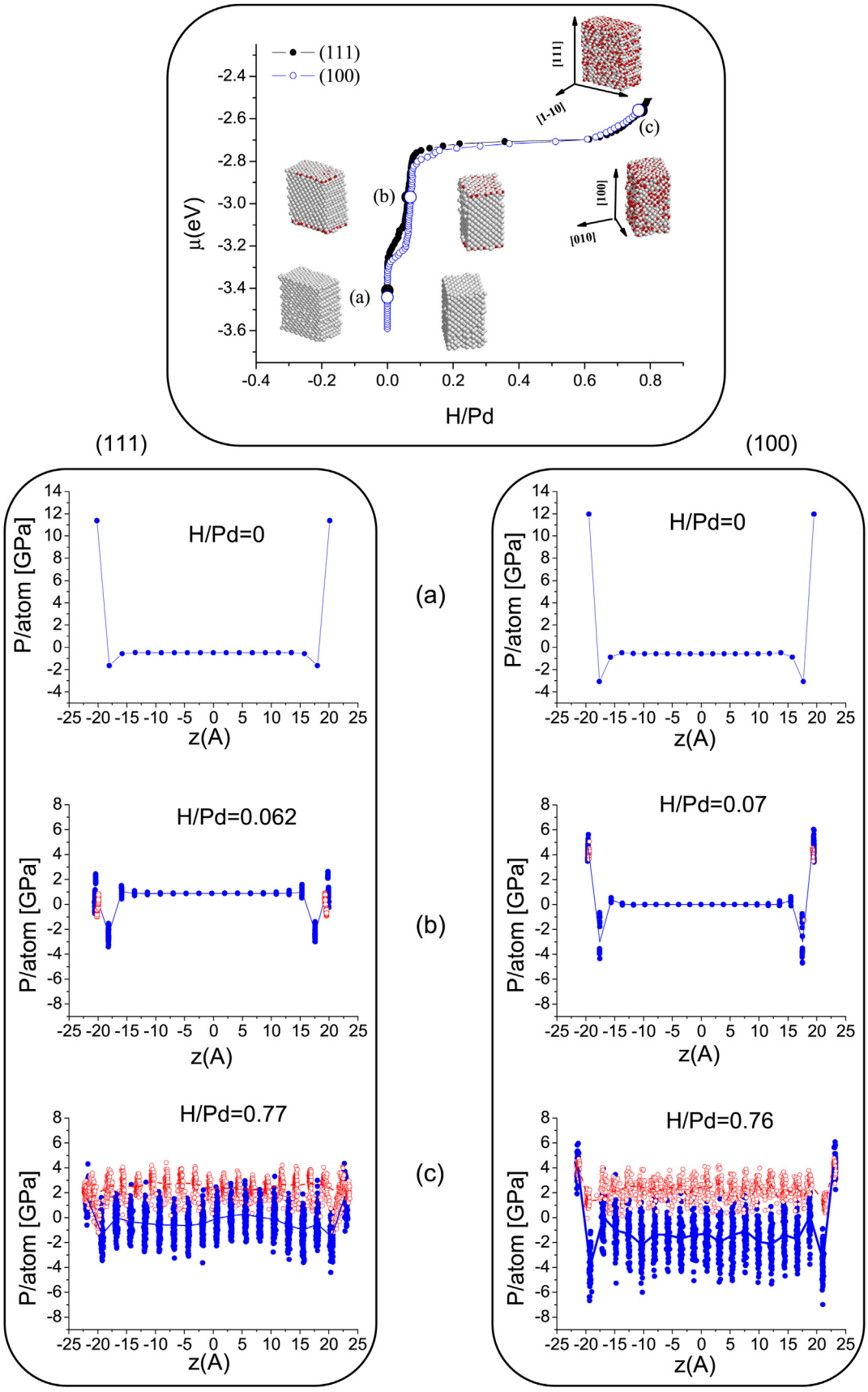

Fig. 1 – Absorption isotherms at 300 K for 4 nm-thick epitaxial films. Top panel: exposed surfaces in the (111) (filled symbols) and (100) (open symbols) directions. Inserts depict atomistic configurations at H/Pd concentrations of approximately (a) = 0, (b) = 0.06 and (c) = 0.76, as shown in panels below, with pressure per atom along the film thickness. H atoms: red, Pd atoms: blue. Lines correspond to average atomic pressure for Pd as discussed in the text. (For interpretation of the references to color in this figure legend, the reader is referred to the web version of this article.)

hydrogen concentration, which is then used to obtain the μ_H–composition isotherm.

The bulk was simulated by considering an initial fcc cell of 864 Pd atoms (6 × 6 × 6) with periodic boundary conditions. The nanofilms (NF) were simulated using epitaxial slabs periodically repeated in the 'x' and 'y' directions, and separated by vacuum. To analyze how the thicknesses of the NF influence the absorption properties, we considered NF of 2, 4, 6 and 8 nm thick. Two different orientations were considered for the surfaces (111) and (001), with exposed areas of 4 × 4 and 6 × 6 unit cells respectively.

We evaluated the atomic stress distribution for different H/Pd selected concentrations in order to analyze the possible correlation between these stresses and the H absorption properties of the nanofilms. The atomic stress tensor of particle 'i' was calculated through the instantaneous virial stress tensor σ [21]:

$$\sigma_i^{\alpha,\beta} = -1/\Omega_i \left[m_i v_i^{\alpha} v_i^{\beta} + \sum_{j \neq i} F_{ij}^{\alpha} r_{ij}^{\beta} \right] \quad (1)$$

where m_i denotes the mass of atom i and Ω_i its atomic volume. Further, v_i, F_{ij}, r_{ij} are the Cartesian components of the atom's velocity, the force between atom i and j and their distance vector, respectively. With this definition, tensile stress is positive and compressive stress negative.

We used the bulk and NF samples generated by our MC simulations at different H concentrations, quenched the samples a $T = 0$ K using the freeware molecular dynamics (MD) code LAMMPS (www.lammps.sandia.gov) [22], and then evaluated the atomic stresses. From the first invariant of the instantaneous stress tensor we calculated the local pressure $p_i = \mathrm{Tr}\sigma/3$. We neglected the thermal contribution, given by the first term in Eq. (1), since its contribution is small at the studied temperatures. It is straightforward to calculate the product of the atomic stress times the atomic volume Ω_i, and this is in fact the output given by LAMMPS. However, to calculate the atomic stress and local pressure one needs to define such atomic volume. This is problematic, since an individual atom's volume might not be well defined or easy to compute for defective solids or in the presence of surfaces [21]. Although there are several possibilities to define the atomic volumes, like the Voronoi's tessellation method [23], in the present work we calculated atomic volumes and pressures assuming spherical volumes with Pauling's radii for both elements (Pd metallic radius = 2.466 Å, H^- ionic radius = 2.085 Å) [24]. As discussed in Ref. [16] for the case of isolated nanoparticles, similar trends for the local atomic pressures are obtained by considering both ways of defining the atomic volumes.

3. Results and discussion

3.1. *Hydrogen absorption properties for nanofilms of different crystallographic orientations*

We first analyzed the influence of the crystallographic orientations on the H absorption properties of the epitaxial nanofilms. In Fig. 1 we show the calculated μ_H–composition isotherms at 300 K for the 4 nm thick film at both (100) and (111) exposed surfaces. In both cases we observed that the isotherms present two plateaux, a behavior already observed for isolated nanoparticles [16]. The first plateau at lower equilibrium chemical potentials is more sloped than the second one; it corresponds to hydrogen filling of surface and subsurface layers of β-Pd hydride, as can be seen in Fig. 1 for selected H concentrations. In Table 1 we show the calculated segregation and absorption energies obtained for H absorbed at the surface hollow and octahedral subsurface sites. These energies were calculated by considering films of approximately 15 layers; the final equilibrium hydrogen positions obtained for surface absorption corresponds to hollow sites absorbed in the top layer of the film. We note that the segregation energies calculated for surface sites are in good agreement with those of Ref. [25.] The occurrence of an additional plateau at lower hydrogen chemical potentials in the absorption isotherm can be explained in terms of the segregation energies which show that the absorption of H is more favorable on surface and subsurface sites than in the bulk, as indicated in Table 1. The higher μ_H equilibrium plateau occurs when the β-PdH transformation inside the bulk is completed. When comparing isotherms for both orientation, it can be noted that the first plateau begins to develop at similar H chemical potentials (similar effective hydrogen pressure), but is more sloped for the (111) NF. We tried to correlate these trends observed in the isotherms with the atomic pressure distribution for the atoms in the NF. Results are indicated in the lower part of Fig. 1 for the (111) (left side) and (001) (right side) NFs. For both orientations, at similar low hydrogen content (Fig. 1(b)), the Pd atoms in the center of the NF are slightly compressed, while atoms at the surface layers are under tension. The present results are compatible with computations of surface stresses in metals using EAM and *ab initio* methods which confirm that the surface stress in metals is usually positive (tensile) due to the bond-order behavior of the metallic bond [28 and references within]. The atoms on the (001) surface are only slightly more stressed than on the (111) surface, while atoms at the subsurface layer are more

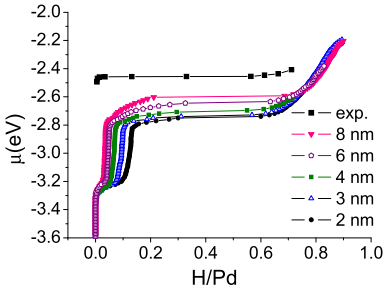

Fig. 2 – Absorption isotherms at 300 K for (001) Pd films with different thicknesses. A small plateau can be seen at low H concentrations corresponding to the formation of a layer of hydride at the surface and subsurface, which tends to disappear at larger thicknesses. The second plateau corresponds to the formation of bulk PdHx. As film thickness increases it appears at higher chemical potential.

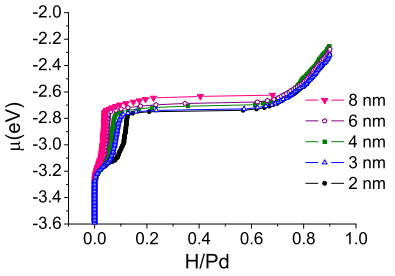

Fig. 3 – Absorption isotherms at 300 K for (111) Pd films with different thicknesses. A small plateau can be seen at low H concentrations corresponding to the formation of a layer of hydride at the surface and subsurface, which tends to disappear at larger thicknesses. The second plateau corresponds to the formation of bulk PdH_x. For thicker films it appears at higher chemical potential.

compressed on the (001) NF. The first plateau forms at similar hydrogen chemical potentials (similar H pressures) for both orientations. As shown in Table 1 both at low coverage (θ = H atoms/Pd surface atoms = 0.0018) and at $\theta = 1$ the calculated absorption energies at a hollow surface site differs by only 0.08 eV, favoring the absorption on the (111) film in qualitative agreement with the *ab initio* results of [27]. We can see that for the (111) NF the first plateau is somewhat more "sloped"; a result that is consistent to the expected higher relative decrease of the binding energy of hydrogen for higher surface coverage at the (111) NF with respect to the (001) one. In fact hydrogen atoms are expected to repel more strongly at the (111) surface than for the (001) one, since this surface can allocate a higher H concentration, as has been confirmed by *ab initio* density functional calculations [26]. We also note that, for low H content (Fig. 1(b)) in the (001) NF, the H atoms are preferentially located on the surface; while on the (111) NF subsurface sites are preferentially occupied. These results can be interpreted in terms of the calculated absorption energies which indicate that for the (111) oriented slab the absorption energies for the surface and subsurface layers are practically the same, with surface sites only slightly more stable (by 0.01 eV) than subsurface sites. For the (001) slab however, the absorption on a surface hollow site is favored by approximately 0.3 eV with respect to the subsurface absorption, therefore explaining the preferential occupation of surface sites by H. From the atomic pressure plots it can be seen that the average stress per atom on the Pd surface atoms (Fig. 1(a)) is lowered by the presence of H atoms (Fig. 1(b)). The absorption of H in the bulk of the NF starts at almost the same chemical potentials for both orientations but, for concentrations of H/Pd higher that approximately 60%, the (001) isotherm crosses over the (111) one, in correlation with the slightly higher average compressive pressure observed for bulk atoms in the (001) NF (Fig. 1(c)). Although not shown in Fig. 1, similar trends are obtained for NFs with different thickness.

3.2. *Hydrogen absorption properties for nanofilms of different thicknesses*

Next we analyzed the influence of the thickness of the NFs in their calculated μ_H–composition isotherms. The isotherms for the different NF thicknesses calculated for the (001) and (111) orientations are shown on Figs. 2 and 3, respectively. Similar general trends as discussed above for the 4 nm NF can be observed. As the thickness increases, the chemical potential at which the first 'surface' plateau appears is practically the same; however the range of H compositions associated to this transformation (the width of the plateau) reduces as the thickness increases in correlation with the decrease of the surface to volume ratio for larger thicknesses, and tends to disappear in the bulk limit as expected. The average chemical potential at which the 'bulk' plateau develops increases with the NF thickness towards the bulk limiting values. The increase in the average chemical potential connected with the 'bulk' plateau is correlated with an average increase in the compressive pressure of the Pd atoms in the inner layers of the NF, as shown in Fig. 4 for the (111) NF at a high H/Pd concentration.

Our results compare qualitatively well with experiments [12,13]. Slightly sloped, narrower plateaux are obtained experimentally for thinner films, as we can observe in our simulations. In Fig. 1 we can see a calculated and experimental bulk isotherm, and the agreement is good. However, we do not see the first calculated plateau in experiments, probably because these are performed on thicker NF in which this effect tends to disappear. The hysteresis effect observed experimentally that tends to be smaller on thinner films

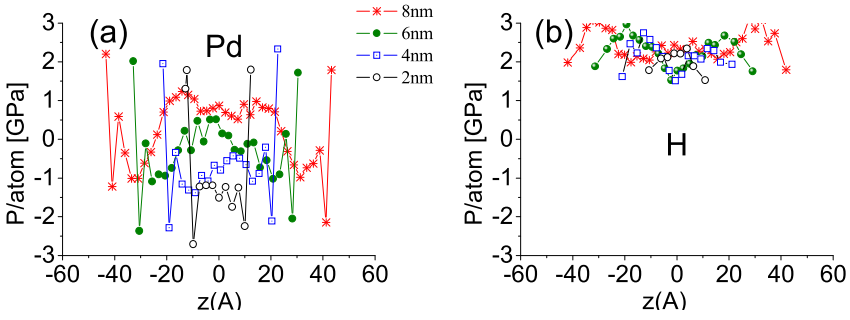

Fig. 4 – Pressure per atom along the film thickness for H/Pd ~ 0.76 and exposed surfaces in the (111) crystallographic direction. a) Pd atoms pressure at different nanofilm thicknesses and b) H atoms pressure at different nanofilm thicknesses.

[12,13] was also simulated by us and the results (not shown here) follow a similar trend.

4. Conclusions

We have performed EAM atomistic simulations to study the effects of thickness and stress distribution on the hydrogen absorption properties of Pd unsupported monocrystalline nanofilms with two crystallographic orientations: (111) and (001). We found that hydrogen absorption properties are sensitive to the nanofilm's thicknesses and to the orientation of their exposed surfaces, as was evidenced by comparing the calculated μ_H-isotherms. In the monocrystalline NFs H was first absorbed on surface and subsurface sites. This was shown as a shoulder or smaller plateau in the μ_H-isotherm for low hydrogen concentrations which is related to a surface hydride transformation. The atomic stress for the surface atoms was tensile, favoring the surface hydrogen absorption. For the (111) NF this plateau was more sloped than for the (001) oriented one. As the thicknesses of the NF increases this first plateau tends to disappear. Higher values of μ_H (higher effective hydrogen pressures) are required for the hydride formation in the inner 'bulk' layers, which is related to the second plateau. The isotherms evolve with NF's thickness towards the bulk limiting isotherm.

Acknowledgments

This work was supported by Universidad Nacional del Comahue Project FAIN No I157. We also thank the Inter U program. E.M. Bringa thanks PICT 2009-0092 and a grant SeCTyP 2011-2013.

REFERENCES

[1] Pundt A, Kirchheim R. Hydrogen in metals: microstructural aspects. Annu Rev Mater Res 2006;36:555–608.
[2] Favier F, Walter EC, Zach MP, Benter T, Penner RM. Hydrogen sensors and switches from electrodeposited palladium mesowire arrays. Science 2001;293:2227–31.
[3] Jewell LL, Davis BH. Review of absorption and adsorption in the hydrogen/palladium system. Appl Catal A 2006;310:1–15.
[4] Antolini E. Palladium in fuel cell catalysis. Energy Environ Sci 2009;2:915–31.
[5] Wolf D. Surface stress induced structure and elastic behavior of thin films. Appl Phys Lett 1991;58:2081–3.
[6] Streitz FH, Cammarata RC, Sieradzki K. Surface-stress on elastic properties. I. Thin metal films. Phys Rev B 1994;49:10699–706.
[7] Hasmy A, Medina E. Thickness induced structural transition in suspended fcc metal films. Phys Rev Lett 2002;88:096103.
[8] Fiorentini V, Methfessel M, Scheffler M. Reconstruction mechanism of fcc transition metal (001) surfaces. Phys Rev Lett 1993;71:1051.
[9] Alefeld G, Volkl J, editors. Topics in applied physics. Hydrogen in metals I, vol. 28. Berlin/Heidelberg/New York: Springer-Verlag; 1978.
[10] Gremaud R, Gonzalez-Silveira M, Pivak Y, de Man S, Slaman M, Schreuders H, et al. Hydrogenography of PdHx thin films: influence of H-induced stress relaxation processes. Acta Mater 2009;57:1209–19.
[11] Cizek J, Melikhova O, Vlcek M, Lukác F, Vlach M, Procázka I, et al. Hydrogen-induced microstructural changes of Pd films. Int J Hydrogen Energy 2013;38(27):12115–25.
[12] Feenstra R, de Groot DG, Rector JH, Salomons E, Griessen R. Gravimetrical determination of pressure-composition isotherms of thin PdHc films. J Phys F Met Phys 1986;16:1953–63.
[13] Pivak Y, Schreuders H, Slaman M, Griessen R, Dam B. Thermodynamics, stress release and hysteresis behavior in highly adhesive Pd-H films. Int J Hydrogen Energy 2011;36:4056–67.
[14] Crespo EA, Claramonte S, Ruda M, Ramos de Debiaggi S. Thermodynamics of hydrogen in Pd nanoparticles. Int J Hydrogen Energy 2010;35:6037–41.
[15] Ruda M, Crespo EA, Ramos de Debiaggi S. Atomistic modeling of H absorption in Pd nanoparticles. J Alloys Compd 2010;495:471–5.
[16] Crespo EA, Ruda M, Ramos de Debiaggi S, Bringa E, Braschi F, Bertolino G. Hydrogen absorption in Pd nanoparticles of different shapes. Int J Hydrogen Energy 2012;37:14831–7.
[17] Zhou XW, Zimmerman JA, Wong BM, Hoyt JJ. An embedded-atom method interatomic potential for Pd-H alloys. J Mater Res 2008;23:704–18.
[18] Wolf R, Lee MW, Davis RC, Fay PJ, Ray JR. Pressure-composition isotherms for palladium hydride. Phys Rev B 1993;48(17):12415–8.
[19] Lee MW, Wolf RJ, Ray JR. Atomistic calculations of hydrogen loading in palladium. J Alloys Compd 1995;231:343–6.
[20] Fukai Y. The metal-hydrogen system. Basic bulk properties. Springer-Verlag. Springer Series in Materials Science; 1993.
[21] Branicio PS, Srolovitz DJ. Local stress calculation in simulations of multicomponent systems. J Comput Phys 2009;228:8467–79.
[22] Plimpton SJ. Fast parallel algorithms for short-range molecular dynamics. J Comput Phys 1995;117:1–19.
[23] Dut Q, Fabert V, Gunzburg M. Centroidal Voronoi tessellations: applications and algorithms. Siam Rev 1999;41:637–76.
[24] Pauling L. The nature of the chemical bond. 10th ed. Cornell University Press; 1955.
[25] Foiles SM, Baskes MI, Daw MS. Embedded-atom method functions for the fcc metals Cu, Ag, Au, Ni, Pd, Pt, and their alloys. Phys Rev B 1986;33:7983–91.
[26] Dong W, Ledentu V, Sautet Ph, Eichler A, Hafner J. Hydrogen adsorption on palladium: a comparative theoretical study of different surfaces. Surf Sci 1998;411:123–36.
[27] Ferrin P, Kando S, Nilekar AU, Mavrilakis M. Hydrogen adsorption, absorption and diffusion on and in transition metal surfaces: a DFT study. Surf Sci 2012;606:679–89.
[28] Diehm PM, Agoston P, Albe K. Size-dependent lattice expansion in nanoparticles: reality or anomaly? ChemPhysChem 2012;13:2443–54.